

Theoretical Prediction of Mass Transfer Coefficients in a Slurry Bubble Column Operated in the Homogeneous Regime

S. Nedeltchev* and A. Schumpe**

Institute of Chemical Engineering, Bulgarian Academy of Sciences,
“Acad. G. Bontchev” Str. Bl. 103, 1113 Sofia, Bulgaria

**Institute of Technical Chemistry, Braunschweig Technical University,
Hans-Sommer-Str. 10, 38106 Braunschweig, Germany

Original scientific paper
Received: August 2, 2007
Accepted: October 15, 2007

The classical penetration theory was corrected and then applied for the semi-theoretical prediction of mass transfer coefficients $k_L a$ in a slurry bubble column operated in the homogeneous regime. The gas-liquid contact time was expressed as a ratio of bubble surface to the rate of surface formation. These terms were defined for the case of oblate ellipsoidal bubbles formed under homogeneous flow conditions. Six different liquid/solid systems (water/activated carbon, water/aluminium oxide, tetralin/aluminium oxide, 0.8 M sodium sulfate solution/kieselguhr (diatomaceous earth), ligroin (petroleum ether)/polyethylene and ligroin/polyvinylchloride) were considered. By means of the same correction factor (a single function of Eötvös number) as derived previously for gas-liquid bubble columns, 85 experimental $k_L a$ values were fitted with a mean error of 19 %.

Key words:

Slurry bubble column, mass transfer, ellipsoidal bubbles, contact time, penetration theory, correction factor

Introduction

Slurry bubble columns (SBCs) are widely used in the chemical and petrochemical industries, e.g., to carry out catalytic hydrogenation or oxidation reactions. SBCs are the preferred type of reactor especially for highly exothermic processes, when efficient interphase contacting is needed and when significant phase backmixing is not detrimental to the operation. These three-phase reactors are characterized with simplicity in construction, low operating cost, excellent heat and mass transfer and variable residence time. SBCs offer several advantages, such as nearly isothermal operation, good interphase contacting, large catalyst area, good productivity, operational flexibility, low pressure drop, possibility of online catalyst addition, low pore diffusion resistance, etc. The SBC is currently the best suited reactor for Fischer-Tropsch synthesis and conversion of natural gas to fuels and chemicals. This reactor type is also considered for both direct and indirect coal liquefaction, waste water treatment as well as biotechnological applications. In SBCs, there is an intense and intimate contact between a gas-phase component, a liquid-phase component and a finely dispersed solid. Usually the catalyst is suspended in the liquid medium by gas-induced agitation at low power consumption. Often in practice

high catalyst loadings are used, and the liquid phase is usually an organic liquid.

Solid particles are used as catalysts, adsorbents, products, or carriers for microorganisms (bacteria, micelles, immobilized enzymes, etc.). In few cases the solid undergoes a reaction in the slurry. An important aspect to be considered in describing the SBC performance is the behavior of solid particles during the reactor operation. A non-uniform distribution of solids along the reactor is likely to develop and it can have a profound effect on the reactor performance. Important variables that influence catalyst distribution and performance of the reactor include particle diameter, particle density, reactor dimensions, liquid and gas velocities. Catalyst particles are usually 10–100 μm in size and pseudo-homogeneously distributed by the action of bubbles. The effect of suspended solids on hydrodynamic properties and on mass transfer at the gas-liquid interface can be extremely complex. Suspension of the catalyst, which normally is of a higher density than the liquid phase, is achieved by the liquid circulation induced by rising bubbles.

Although SBCs are very simple in construction and operation due to the absence of moving parts, their hydrodynamics are complex and a strong function of operating conditions (e.g. pressure, gas velocity), physical properties (liquid viscosity, surface tension) and scale (diameter, height). The SBC performance is strongly dependent on the bubble

*Corresponding author, e-mail: snn13@gmx.net

characteristics (bubble size, bubble rise velocity and bubble wake phenomena). These parameters determine the gas holdup, the interfacial area, the gas residence time and also the liquid mixing. The SBC performance, however, can alter significantly following a change in flow regime. The hydrodynamics and flow patterns in the SBC are complex phenomena, which makes their design and scale-up a difficult task.

The major drawbacks of SBCs are strong backmixing in the bulk of the reactor and complex scale-up (Deckwer¹). Catalyst separation can cause problems in a continuous process, and filter costs can be high as a certain amount of catalyst abrasion occurs during the SBC operation. Recently, Nedeltchev and Schumpe² have systematically covered the subject of SBC technology.

Effect of solids on the mass transfer characteristics ($k_L a$ and gas holdup)

The design and scale-up of SBCs require comprehensive knowledge of the hydrodynamics and mass transfer under various operating conditions. Most of the correlations for SBCs are based on the air-water-glass beads system. Common to nearly all investigations is the finding that the volumetric liquid-side mass transfer coefficient $k_L a$ decreases with the addition of solid particles.^{3–5} The same trend prevails for mechanically agitated reactors;^{6,7} the group of Deckwer⁸ has shown that the effect of solid particles on $k_L a$ depends on solid loading and particle nature. Some additional papers about the effect of solids on $k_L a$ values can be found in Nedeltchev and Schumpe.²

The overall solids effect on $k_L a$ is constituted from the individual effects on k_L and a . Solid particles may enhance the surface renewal frequency at low solid concentrations and thus increase k_L . Nguyen-tien et al.⁹ measured $k_L a$ values in a bubble column varying glass beads concentration and diameter (from 0.05×10^{-3} m to 8×10^{-3} m) using high liquid velocities to fluidize the larger particles. For the particle size of $50 \mu\text{m}$, the $k_L a$ values increase slightly at low solid loadings. At higher concentrations, small solid particles increase the solution viscosity, decrease the turbulence level and enhance the bubble coalescence frequency, which results in a decrease of both k_L and a (Chang and Morsi⁶). Similar results were reported by Deckwer et al.⁷ using sea sand in a gas-sparging agitated reactor. Chang and Morsi⁶ reported that the larger solid particles show slightly higher $k_L a$ values than those obtained with smaller solid particles. This behavior can be explained by the more violent turbulence in the liquid film for larger particles compared to smaller particles. Nagaraj and Gray¹⁰ con-

cluded that smaller particles tend to attach to the bubble wakes and produce a higher bubble coalescence frequency. Consequently, both k_L and a values are expected to decrease.

Mass transfer during Fischer-Tropsch synthesis was also investigated under reactive conditions using a model reaction (CO conversion).¹¹ The $k_L a$ values could not be described by empirical correlations due to the unusually high specific interfacial area found in that particular system.

Luo et al.¹² found that gas holdup increases with an increase in pressure, especially at high slurry concentrations. The pressure effect is more pronounced at low pressures and higher solids concentrations. The scale effect on the gas holdup is relatively small at high pressures due to the smaller bubble sizes. The gas holdup is basically dictated by the size and rise velocity of bubbles. Luo et al.¹² reported that at ambient pressure, a higher solids concentration significantly lowers gas holdup over the entire gas velocity range, while at 5.6 MPa, the effect of solids concentration on gas holdup is relatively small at gas velocities above 0.25 m s^{-1} . An empirical correlation was developed based on a large database to predict gas holdup in both BCs and SBCs over a wide range of operating conditions. Bubble size increases significantly with increasing solids concentration at ambient pressure, while at high pressures this effect is less pronounced. Luo et al.¹² argue that the particle size effect on the gas holdup can be neglected in the particle-size range of $44\text{--}254 \mu\text{m}$.

Some empirical correlations for $k_L a$ prediction

No general mass transfer correlation exists for the design of SBCs. The performance of these reactors largely depends on the characteristics of the employed particles (size, density, shape, wetting properties, etc.). Therefore, it is doubtful whether the results from one model system could be transferred to other systems. Recently, Nedeltchev and Schumpe² have summarized the most important $k_L a$ correlations for SBCs.

Öztürk and Schumpe¹³ measured $k_L a$ in a 0.095 m inner diameter bubble column absorbing oxygen in organic liquids containing up to 40 % of various polymer particles and aluminum oxide. With the exception of high-density particles in a low viscosity liquid (alumina in ligroin (petroleum ether)), all results could be uniformly correlated (mean error: 7.7 %):

$$\frac{k_L a}{(k_L a)_0} = \left(\frac{\mu_{\text{eff}}}{\mu_{L0}} \right)^{-0.42} \quad (1)$$

The correlation covers u_G values up to 0.08 m s⁻¹ and an effective viscosity range of 0.54–100 × 10⁻³ Pa s. The subscript 0 refers to the same operating conditions without solids. Öztürk and Schumpe¹³ reported that small concentrations of fine high density particles (8 μm aluminium oxide, 7 μm kieselguhr (diatomaceous earth)) slightly increased the k_L value. This increase is limited to relative viscosities μ_{eff}/μ_L less than 2. The positive effect of fine high density solids on $k_L a$ has been attributed to a hydrodynamic effect on k_L by particle penetration into the liquid-side diffusion film.⁹ Öztürk and Schumpe¹³ concluded that it is essentially the effective suspension viscosity which determines the performance of the SBC.

For aqueous slurries (water and aqueous salt solutions with kieselguhr, alumina and activated carbon), Schumpe et al.¹⁴ found a very similar viscosity effect:

$$\frac{k_L a}{(k_L a)_0} = \left(\frac{\mu_{eff}}{\mu_{L0}} \right)^{-0.39} \quad (2)$$

Eq. (2) is valid for $u_G < 0.08$ m s⁻¹ and $1 < \mu_{eff} < 100 \times 10^{-3}$ Pa s.

Fine high-density solids in low-viscous liquids such as alumina in ligroin or kieselguhr in water (at low concentration) yield slightly higher $k_L a$ values than predicted by Eqs. (1) or (2), possibly by higher k_L (Schumpe et al.¹⁴). However, non-wettable particles may reduce $k_L a$ much stronger than predicted by Eqs. (1) and (2).

Nigam and Schumpe¹⁵ found that the relation developed for three-phase fluidized beds of glass spheres in the group of Deckwer⁹

$$\frac{k_L a}{(k_L a)_0} = \left(1 - \frac{\phi_s}{0.58} \right) \quad (3)$$

is also applicable to SBCs with non-uniform distribution of the particles ($5 < d_p < 200$ μm). However, the solids fraction ϕ_s at the bottom (where intense coalescence occurs) should be substituted into Eq. (3). The solids fraction ϕ_s could be measured or calculated with the sedimentation-dispersion model.

Correction of Higbie's penetration theory

For gas-liquid bubble columns operated in the homogeneous flow regime, Nedeltchev et al.^{16–18} developed a correction of Higbie's penetration theory¹⁹ for the case of oblate ellipsoidal bubbles. There are two important steps in this correction procedure. The first involves a proper definition of

gas-liquid contact time t_c which takes part in the correlation of the liquid-phase mass transfer coefficient k_L :

$$k_L = \sqrt{\frac{4D_L}{\pi t_c}} \quad (4)$$

Nedeltchev et al.^{16–18} defined the characteristic time t_c as follows:

$$t_c = \frac{\text{Bubble surface}}{\text{Rate of surface formation}} \quad (5)$$

In the case of oblate ellipsoidal bubbles, the bubble surface S_B and the rate of surface formation R_{sf} can be defined as follows:

$$S_B = \pi \frac{l^2}{2} \left[1 + \left(\frac{h}{l} \right)^2 \frac{1}{2e} \ln \frac{(1+e)}{(1-e)} \right] \quad (6)$$

where the eccentricity e is

$$e = \sqrt{1 - \left(\frac{h}{l} \right)^2} \quad (6a)$$

$$R_{sf} = \pi \sqrt{\frac{l^2 + h^2}{2} - \frac{(l-h)^2}{8}} u_B \quad (7)$$

In this approach, the correct estimation of bubble length l and bubble height h of the ellipsoidal bubbles is crucial. Both geometrical characteristics of the ellipsoidal bubble were calculated by means of the formulas derived by Terasaka et al.²⁰. It is worth noting that the behavior of multi-bubbles is complex. The oblate ellipsoidal bubble shape was verified by means of the bubble shape diagram (logarithmic values of the bubble Reynolds number vs. logarithmic values of the Eötvös number at various Morton numbers) developed by Fan and Tsuchiya²¹. The expression for the rate of surface formation involves also the bubble rise velocity u_B which was calculated by means of Mendelson's correlation²² derived from the wave theory. According to Painmanakul et al.²³ the specific interfacial area a can be calculated from the number of bubbles N_B , the bubble surface S_B and the dispersion volume:

$$a = \frac{N_B S_B}{AH} = \frac{f_B S_B}{A u_B} \quad (8)$$

where A is the cross-sectional area and H is the dispersion height.

Nedeltchev et al.¹⁶ found that the $k_L a$ values for ellipsoidal bubbles should be calculated by means of the following formula:

$$k_L a = f_c \sqrt{\frac{4D_L R_{sf}}{\pi S_B}} \frac{f_B S_B}{A u_B} \quad (9)$$

where the correction factor for oblate ellipsoidal bubbles was expressed as follows:

$$f_c = 0.185 Eo^{0.737} = 0.185 \left(\frac{g(\rho_L - \rho_G)d_e^2}{\sigma} \right)^{0.737} \quad (10)$$

This correction factor was derived based on 79 $k_L a$ values obtained in 14 organic liquids and tap water¹⁶. The average relative error was 8.7 %.

The equivalent bubble size d_e was calculated as follows:

$$d_e = (l^2 h)^{1/3} \quad (11)$$

Both bubble length l and bubble height h are functions of the Tadaki number and the equivalent bubble diameter d_e (see Terasaka et al.²⁰) and these parameters have been estimated based on the correlation for the Sauter-mean bubble diameter d_s proposed by Wilkinson et al.²⁴

$$\left(\frac{g \rho_L d_s^2}{\sigma} \right) = 8.8 \left(\frac{u_G \mu_L}{\sigma} \right)^{-0.04} \left(\frac{\sigma^3 \rho_L}{g \mu_L^4} \right)^{-0.12} \left(\frac{\rho_L}{\rho_G} \right)^{0.22} \quad (12)$$

More details about the calculation of both l and h values from d_s and d_e can be found in Nedeltchev et al.^{16–18} The mean bubble diameter decreases with increasing gas density or pressure. However, above a certain pressure, the bubble size reduction is not significant. The effect of pressure on the mean bubble size is due to the change of bubble size distribution with pressure.

The objective of this paper is to check whether the correction factor f_c (see Eq. 10) derived in the case of gas-liquid bubble columns can be applied successfully for the sake of theoretical prediction of the $k_L a$ values in SBCs operated in the homogeneous regime at low solids fractions.

Experimental data considered

The considered mass transfer measurements^{13,14} were carried out in a glass bubble column of 0.095 m diameter at a height of the gas-free suspensions of 0.85 m. The slurries were operated batchwise. The air flow rate was controlled with a mass flow meter. Prior to entering the column, the gas was passed through a saturator filled with the same liquid at the same temperature. Tetralin and ligroin (petroleum ether, b.p. range 373–413 K) were aerated through a single tube of 3×10^{-3} m inner diameter; for tap water and 0.8 M Na₂SO₄ a single tube of 0.9×10^{-3} m inner diameter was employed as the gas distributor. Four different liquids have been used and their physicochemical properties are listed in Table 1.

The solid particles used in tap water were activated carbon ($\rho_s=1800$ kg m⁻³, $d_p=5.4$ μm) and aluminium oxide ($\rho_s=3180$ kg m⁻³, $d_p=8.1$ μm). In the sodium sulfate solution, kieselguhr (diatomaceous earth) particles ($\rho_s=2360$ kg m⁻³, $d_p=6.6$ μm) were suspended. Aluminium oxide particles ($\rho_s=3180$ kg m⁻³, $d_p=10.5$ μm) were studied in tetralin and both polyethylene (B) particles ($\rho_s=965$ kg m⁻³, $d_p=106$ μm) and polyvinylchloride (PVC) particles ($\rho_s=1380$ kg m⁻³, $d_p=82$ μm) were introduced into ligroin. Superficial gas velocities u_G in the range of 0.016 to 0.04 m s⁻¹ (homogeneous flow regime according to the formulas of Reilly et al.²⁵ based on the slurry density ρ_{SL}) were considered.

The gas holdups were determined from the change in dispersion height due to the gas flow. The volumetric mass transfer coefficients $k_L a$ were investigated by the dynamic oxygen absorption method, i.e. the increase in oxygen fugacity during aeration of the initially oxygen-free liquids was measured with a fast response polarographic oxygen electrode (WTW EO 90, time constant: 3 s). First, oxygen was desorbed by sparging nitrogen. After disengagement of the nitrogen bubbles but before any significant sedimentation of the particles, aeration was started by switching two magnet

Table 1 – Physicochemical properties of the liquids used

Liquid	T [K]	μ_L [10 ⁻³ Pa s]	ρ_L [kg m ⁻³]	σ [10 ⁻³ N m ⁻¹]	D_L [10 ⁻⁹ m ² s ⁻¹]
Tap water	298.2	0.89	997	72.7	2.1
0.8 M Na ₂ SO ₄	298.2	1.26	1095	75.0	1.6
Ligroin	293.2	0.54	729	21.4	3.6
Tetralin	293.2	2.08	968	34.9	1.55

valves. More details are given in the original papers.^{13,14} Since in the case of very viscous slurries there is hardly any homogeneous flow regime, the solids fraction ϕ_s was limited to values below 0.1.

Results and discussion

The main problem when one tries to apply the correction method (section 2) to SBCs is how to calculate the bubble size. In the presence of solid particles, as a first approximation, it can be assumed that the particles modify only homogeneous properties of the surrounding medium.²⁶ Zhao and Ge²⁷ treated the solids and the liquid phase as a homogeneous mixture. According to these authors, the liquid-solid suspension can be treated as a pseudo-homogeneous medium especially when the particle size is much smaller than the bubble size and the concentration of the solids is not too high. Rados et al.²⁸ argue that SBCs are most often modeled as two-phase gas-slurry systems. Considering the fairly small size of the solid particles that are typically used in SBCs (mean size below 50 μm), most authors agree that the pseudo-homogeneous slurry assumption is probably reasonable.

Based on this homogeneous approach,²⁶ the equations for gas-liquid systems can be extended to liquid-solid suspensions by replacing the liquid properties ρ_L and μ_L with the effective properties of the liquid-solid suspension ρ_{SL} and μ_{eff} , respectively. The effective density can be estimated as follows:

$$\rho_{SL} = \rho_L(1 - \phi_s) + \rho_s\phi_s \quad (13)$$

The effective viscosity μ_{eff} of liquid-solid suspensions was calculated from the Ostwald-de Waele relation (eq. 14), where the effective shear rate was estimated by means of Eq. (14a) proposed by Schumpe et al.:^{13,29}

$$\mu_{eff} = k \dot{\gamma}^{n-1} \quad (14)$$

$$\dot{\gamma} = 2800 u_G \quad (14a)$$

The values of k and n for the suspensions were taken from Öztürk and Schumpe¹³ and Schumpe et al.,¹⁴ respectively. The bubble rise velocity u_B was estimated by means of Mendelson's correlation²² substituting the liquid density ρ_L with the slurry density ρ_{SL} . In the process of estimation of both geometrical characteristics (length and height) of ellipsoidal bubbles, the Tadaki number Ta was defined on the basis of the the slurry density ρ_{SL} and the effective viscosity μ_{eff} . The experimental $k_L a$ values fall in both ranges ($2 < Ta < 6$ and $6 < Ta < 16.5$) specified by Terasaka et al.²⁰

In the case of SBCs, the Eo expression (Eq. 10) should be based on slurry density ρ_{SL} instead of

liquid density ρ_L . It is worth noting that there was no fitting of the correction factor to the present data set. Fig. 1 shows that in the case of three different gas-liquid-solid systems (45 $k_L a$ values) the correction factor (Eq. 10) can be applied successfully for $k_L a$ prediction in SBCs. In the case of air-water-activated carbon system the solids fraction in the gas-free suspension ϕ_s ranged from 0.026 to 0.051 and for air-water-aluminium oxide system the ϕ_s values ranged from 0.016 to 0.063. In the case of air-ligroin-PE (B) system also low solids fractions ϕ_s in the range of 0.012-0.074 were used. Fig. 1 shows that for air-water-aluminium oxide system for solids fractions ϕ_s up to 0.031 the experimental $k_L a$ values at low u_G values are about 25 % higher than the theoretically calculated ones. This trend might be explained by the k_L increase due to particles penetrating the diffusion film.

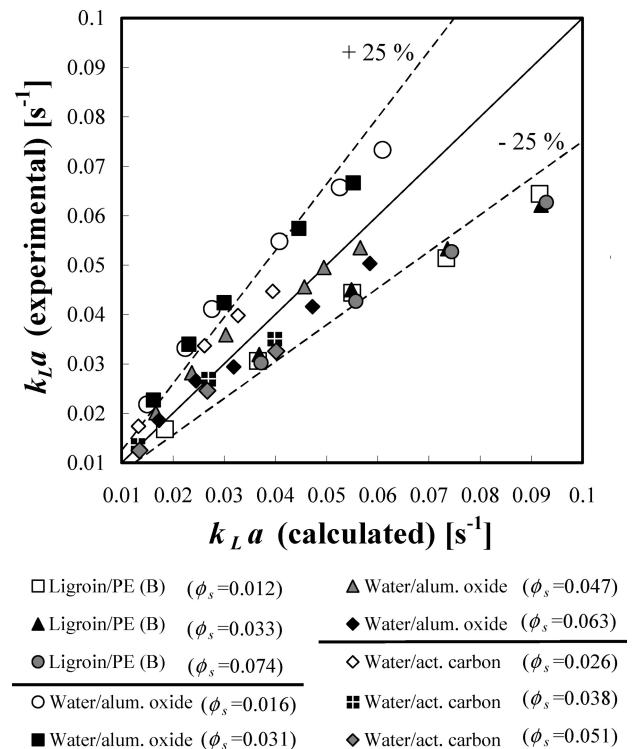


Fig. 1 – Parity plot of $k_L a$ values measured in a SBC operated with air-ligroin-polyethylene (B) (PE(B)), air-water-aluminium oxide and air-water-activated carbon systems

Fig. 2 illustrates the successful application of the common correction term, Eq. (10) based on ρ_{SL} , to three additional gas-liquid-solid systems (40 $k_L a$ values). In the case of the air-ligroin-PVC system, ϕ_s values up to 0.053 were tested, whereas for air-tetralin-aluminium oxide system ϕ_s values up to 0.056 were examined. In the case of air-sodium sulfate-kieselguhr system only one ϕ_s value (0.085) was fitted satisfactorily.

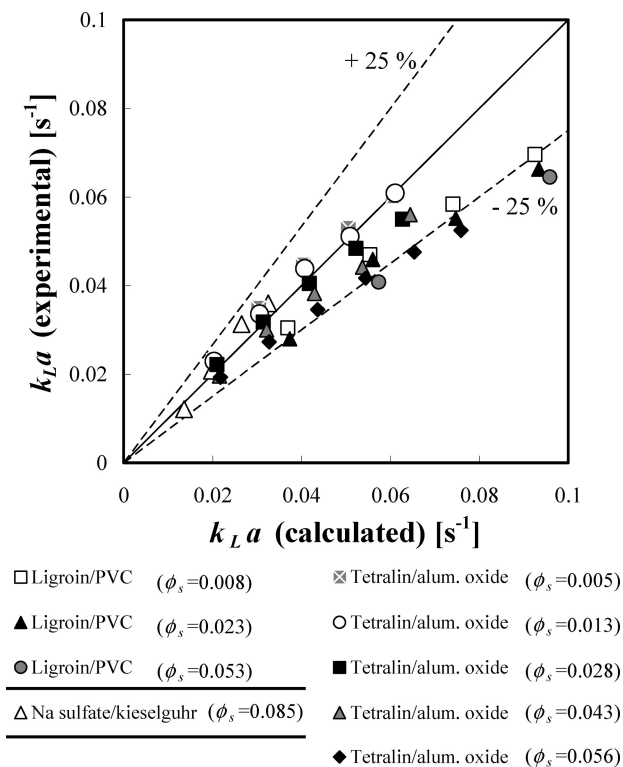


Fig. 2 – Parity plot of $k_L a$ values measured in a SBC operated with three additional gas-liquid-solid systems at low solids fractions

Schumpe et al.¹⁴ found that the addition of kieselguhr (diatomaceous earth) leads to a significant $k_L a$ increase in the lower concentration range. Low concentrations of fine high density solids like kieselguhr (and aluminium oxide) increase the k_L value by a hydrodynamic effect on the liquid film around the bubbles. This positive effect is limited to relative viscosities less than about 2. It is obvious that this cannot be described with a pseudo-homogeneous approach. Only at the kieselguhr concentration of 100 kg m^{-3} the $k_L a$ values start to become smaller than in the two-phase system. This corresponds to the beginning of a rather steep increase in viscosity with concentration and the development of non-Newtonian flow behavior. In the highly viscous kieselguhr slurries the k_L values are smaller than in the two-phase system. This trend has also been observed by Sada et al.³⁰. Schumpe et al.¹⁴ reported that except for the low concentrated kieselguhr slurries (solid loadings below 100 kg m^{-3}) all other $k_L a$ values can be uniformly correlated by the effective viscosity μ_{eff} .

In Figs. 1 and 2 the calculated $k_L a$ values which are above 0.05 s^{-1} are over 25 % higher than the experimental $k_L a$ values. A reasonable explanation for this trend might be that, at high bubble density, different bubble classes begin to form in the bubble bed (transition to heterogeneous flow).

Fig. 3 shows that in the case of four different gas-liquid-solid systems the correction factor f_c derived by Nedeltchev et al.¹⁶ for gas-liquid bubble columns is very close to the one derived by Wellek et al.³¹ The latter shows to what extent the shape of the actual bubble deviates from the spherical shape. At Eo values above 10 the correction factor f_c becomes higher than unity. This occurs only in the case of air-water-aluminium oxide system at $\phi_s=0.063$. Under this particular condition, the largest bubbles are formed which are characterized with the biggest wakes. The latter enhance the mass transfer coefficients and that is why the correction factor f_c becomes somewhat higher than unity.

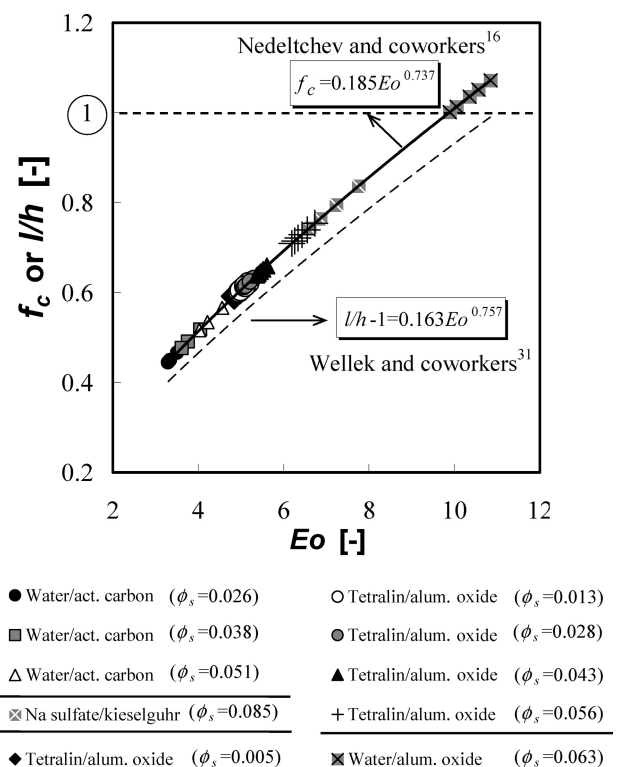


Fig. 3 – Dependence of the correction factor f_c on the Eötvös number Eo in the case of four gas-liquid-solid systems operated with different low solids fractions ϕ_s

The presented results demonstrate that under homogeneous flow conditions a unified correction of the penetration theory valid for both gas-liquid bubble columns and SBCs (operated at low solids fractions ϕ_s) could be successfully applied.

Conclusion

For solid fractions ϕ_s smaller than 0.1 the correction of the penetration theory derived for homogeneous gas-liquid dispersions can be applied successfully for theoretical prediction of the volumet-

ric mass transfer coefficients $k_L a$ in SBCs operated in the homogeneous regime at low solids fractions. In this approach, only liquid density and liquid viscosity must be substituted by slurry density and effective slurry viscosity in the key correlations for the estimation of bubble shape characteristics and bubble rise velocity. By means of the common correction factor, 85 experimental $k_L a$ values measured in a SBC operated with six different gas-liquid-solid systems at solids fractions ϕ_s up to 0.1 were fitted satisfactorily with an average relative error of 19 %. This somewhat high value can be explained by the fact that the correction factor derived for gas-liquid bubble columns was directly applied to SBCs without any modification although the present data set is larger. The proposed mass transfer model predicts satisfactorily the experimental $k_L a$ data necessary for reliable scale up, process optimization and prediction of the performance of SBCs operated in the homogeneous flow regime at low solids fractions.

ACKNOWLEDGEMENT

Dr. Stoyan Nedeltchev is grateful to the Alexander von Humboldt Foundation (Germany) for the Postdoctoral Fellowship (2005 – 2007).

Nomenclature

a	– gas-liquid interfacial area, m^{-1}
A	– column cross-section, m^2
D_L	– oxygen molecular diffusivity in the liquid, $\text{m}^2 \text{s}^{-1}$
d_e	– equivalent bubble diameter, m
d_p	– mean particle diameter, m
d_s	– Sauter-mean bubble diameter, m
e	– bubble eccentricity, dimensionless
f_B	– bubble formation frequency, s^{-1}
f_c	– correction factor, dimensionless
g	– acceleration due to gravity, m s^{-2}
h	– height of an ellipsoidal bubble, m
H	– dispersion height, m
k	– fluid consistency index, Pa s^n
k_L	– liquid-phase mass transfer coefficient, m s^{-1}
$k_L a$	– volumetric mass transfer coefficient (referred to slurry gas/liquid/solid volume), s^{-1}
l	– length (width) of an ellipsoidal bubble, m
n	– flow behavior index, dimensionless
N_B	– number of bubbles in gas-liquid-solid dispersion, dimensionless
R_{sf}	– rate of surface formation, $\text{m}^2 \text{s}^{-1}$
S_B	– bubble surface, m^2
t_c	– gas-liquid contact time, s
u_B	– bubble rise velocity, m s^{-1}
u_G	– superficial gas velocity, m s^{-1}

Greek letters

ϕ_s	– solids fraction in the gas-free suspension, dimensionless
γ	– effective shear rate, s^{-1}
μ_{eff}	– apparent (effective) viscosity of liquid-solid suspension, Pa s
μ_L	– liquid viscosity, Pa s
ρ_G	– gas density, kg m^{-3}
ρ_L	– liquid density, kg m^{-3}
ρ_S	– solid density, kg m^{-3}
ρ_{SL}	– slurry density (density of liquid-solid suspension), kg m^{-3}
σ	– surface tension, N m^{-1}

Dimensionless numbers

Eu	– Eötvös number, dimensionless
Ta	– Tadaki number, dimensionless

Index

0	– refers to the solid-free system
---	-----------------------------------

Abbreviation

SBC – slurry bubble column

References

1. Deckwer, W.-D., *Bubble Column Reactors*, John Wiley, New York, 1992.
2. Nedeltchev, S., Schumpe, A., Chapter 10.3: Slurry Reactors, in Ertl, G., Knözinger, H., Schüth, F., Weitkamp, J. (Ed.), *Handbook of Heterogeneous Catalysis*, Wiley-VCH, Weinheim, 2008 (in press).
3. Sauer, T., Hempel, D.-C., *Chem. Eng. Tech.* **10** (1987) 180.
4. Koide, K., Takazawa, A., Komura, M., Matsunaga, H., *J. Chem. Eng. Japan* **17** (1984) 459.
5. Schumpe, A., Fang, L. K., Deckwer, W.-D., *Chem.-Ing.-Tech.* **56** (1984) 924.
6. Chang, M.-Y., Morsi, B. I., *Chem. Eng. Sci.* **47** (1992) 1779.
7. Oguz, H., Brehm, A., Deckwer, W.-D., *Chem. Eng. Sci.* **42** (1987) 1815.
8. Alper, E., Wichtendahl, B., Deckwer, W.-D., *Chem. Eng. Sci.* **35** (1980) 217.
9. Nguyen-tien, K., Patwari, A. N., Schumpe, A., Deckwer, W.-D., *AIChE J.* **31** (1985) 194.
10. Nagaraj, N., Gray, D. J., *AIChE J.* **33** (1987) 1563.
11. Deckwer, W.-D., Louisi, Y., Zaidi, A., Ralek, M., *Ind. Eng. Chem. Proc. Des. Dev.* **19** (1980) 699.
12. Luo, X., Lee, D. J., Lau, R., Yang, G., Fan, L.-S., *AIChE J.* **45** (1999) 665.

13. Öztürk, S., Schumpe, A., *Chem. Eng. Sci.* **42** (1987) 1781.
14. Schumpe, A., Saxena, A. K., Fang, L. K., *Chem. Eng. Sci.* **42** (1987) 1787.
15. Nigam, K., Schumpe, A., *AIChE J.* **33** (1987) 328.
16. Nedeltchev, S., Jordan, U., Schumpe, A., *Chem. Eng. Tech.* **29** (2006) 1113.
17. Nedeltchev, S., Jordan, U., Schumpe, A., *J. Chem. Eng. Japan* **39** (2006) 1237.
18. Nedeltchev, S., Jordan, U., Schumpe, A., *Chem. Eng. Sci.* **62** (2007) 6263.
19. Higbie, R., *Trans. Am. Inst. Chem. Eng.* **31** (1935) 365.
20. Terasaka, K., Inoue, Y., Kakizaki, M., Niwa, M., *J. Chem. Eng. Japan* **37** (2004) 921.
21. Fan, L.-S., Tsuchiya, K., *Bubble Wake Dynamics in Liquids and Liquid-Solid Suspensions*, Butterworth-Heinemann, Stoneham, USA, 1990.
22. Mendelson, H. D., *AIChE Journal* **13** (1967) 250.
23. Painmanakul, P., Loubière, K., Hébrard, G., Mietton-Peuchot, M., Roustan, M., *Chem. Eng. Sci.* **60** (2005) 6480.
24. Wilkinson, P. M., Haringa, H., Van Dierendonck, L. L., *Chem. Eng. Sci.* **49** (1994) 1417.
25. Reilly, I. G., Scott, D. S., de Bruijn, T. J. W., MacIntyre, D., *Can. J. Chem. Eng.* **72** (1994) 3.
26. Yang, G. Q., Du, B., Fan, L.-S., *Chem. Eng. Sci.* **62** (2007) 2.
27. Zhao, H., Ge, W., *Chem. Eng. Sci.* **62** (2007) 109.
28. Rados, N., Al-Dahhan, M. H., Dudukovic, M. P., *Ind. Eng. Chem. Res.* **44** (2005) 6086.
29. Schumpe, A., Deckwer, W.-D., *Bioprocess. Engng.* **2** (1987) 79.
30. Sada, E., Kumazawa, H., Lee, C. H., *Chem. Eng. Sci.* **38** (1983) 2047.
31. Wellek, R. M., Agrawal, A. K., Skelland, A. H. P., *AIChE J.* **12** (1966) 854.